

Electronic Supplementary Information

Hexafluorobenzene: a powerful solvent for noncovalent stereoselective organocatalytic Michael addition reaction

Alessandra Lattanzi^{*,a} Claudia De Fusco,^a Alessio Russo,^a Albert Poater^b and Luigi Cavallo^{*,a,c}

^a*Dipartimento di Chimica e Biologia, Università di Salerno, Via Ponte don Melillo, 84084 (I), Fisciano, Italy*

lattanzi@unisa.it; lcavallo@unisa.it

^b*Catalan Institute for Water Research (ICRA), H₂O Building, Scientific and Technological Park of the University of Girona, Emili Grahit 101, E-17003, Girona, Spain*

^c*King Abdullah University of Science and Technology, Thuwal 23955-6900, Kingdom of Saudi Arabia*

Table of contents

General Information.....	S2
Catalysts and Solvents Study (Tables).....	SError! Bookmark not defined.
Experimental Procedures and Compounds Characterization.....	S5
General procedure for synthesis of racemic Michael adducts 4b , 4d , 4e , 4i , 4k	S5
General procedure for the asymmetric conjugate addition.....	S5
HPLC chromatograms of compounds 4b , 4d , 4e , 4i , 4k	S12
Computational Details.....	S17
Gas-phase BP86/TZVP energy of the calculated transition states.....	S17
Steric profiles in transition states pro-R,S and pro-S,R.....	S18

General Information

Diethyl ether were dried over molecular sieves (Aldrich Molecular Sieves, 3 Å, 1.6 mm pellets, activated under vacuum at 200°C overnight). Reactions were monitored by thin layer chromatography (TLC) on Merck silica gel plates (0.25 mm) and visualized by UV light and by I₂ vapors. Flash chromatography was carried out using Merck silica gel (60, particle size: 0.040–0.063 mm). ¹H NMR and ¹³C NMR spectra were recorded on Bruker DRX 400 spectrometer at room temperature in CDCl₃ as solvent. Chemical shifts for protons are reported using residual CHCl₃ as internal reference (δ = 7.26 ppm). Carbon spectra were referenced to the shift of the ¹³C signal of CDCl₃ (δ = 77.0 ppm). Optical rotations were performed on a Jasco Dip-1000 digital polarimeter using the Na lamp.

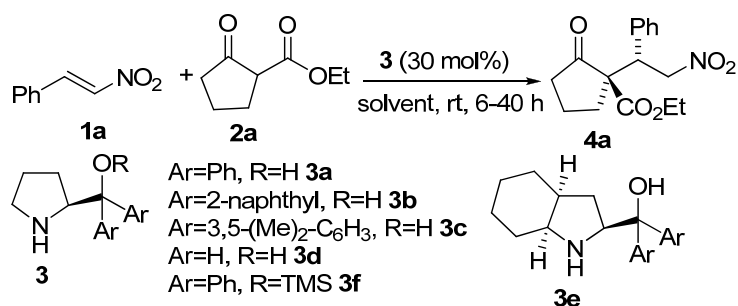
Petrol ether (PE) refers to light petroleum ether (boiling point 40-60 °C). Anhydrous benzene, anhydrous toluene and hexafluorobenzene were purchased from Aldrich. Catalysts **3a-d** and **3f**, β-ketoesters and *trans*-nitrostyrene **1a** are commercially available reagents. They were purchased from Aldrich and used as received. Catalyst **3e** was prepared according to the literature.¹ *Trans*-nitroalkenes **1b-i** were prepared using general procedures reported in the literature.² All Michael adducts are known compounds.³ Enantiomeric excesses were determined by HPLC performed on Waters 2487 instrument, equipped with UV detector and 1525 Binary Pump, using Daicel Chiralpak IC, Chiralpak AS-H, Chiralpak AD-H and Chiralcel OD and OD-H columns.

¹ a) R.-S. Luo, J. Weng, H.-B. Ai, G. Lu, A. S. C. Chan, *Adv. Synth. Catal.* **2009**, *351*, 2449; b) K. M. B. Gross, Y. M. Jun, P. Beak, *J. Org. Chem.* **1997**, *62*, 7679.

² a) O. Andrey, A. Alexakis, G. Belardinelli, *Org. Lett.* **2003**, *5*, 2559; b) A. Côté, V. N. G. Lindsay, A. B. Charette *Org. Lett.* **2007**, *9*, 85.

³ a) For data of compound **4a**, **5** and **6**, see: D. Almaşi, D. Alonso, E. Gómez-Bengoa, C. Nájera, *J. Org. Chem.* **2009**, *74*, 6163; Manzano, R.; Andrés, J. M.; Muruzábal, M.; Pedrosa, R. *Adv. Synth. Cat.* **2010**, *352*, 3364; T. Okino, Y. Hoashi, T. Furukawa, X. Xu, Y. Takemoto *J. Am. Chem. Soc.* **2005**, *127*, 119; b) For data of compounds **4b-f**, see: X. Jiang, Y. Zhang, X. Liu, G. Zhang, L. Lai, L. Wu, J. Zhang, R. Wang, *J. Org. Chem.* **2009**, *74*, 5562; c) For data of compounds **4g-h**, see: K. Murai, S. Fukushima, S. Hayashi, Y. Takahara, H. Fujioka, *Org. Lett.* **2010**, *12*, 964; d) For data of compounds **4i-k** and **5**, see: Z. H. Zhang, X. Dong, D. Chen, C. J. Wang *Chem. Eur. J.* **2008**, *14*, 8780; e) For data of compound **8**, see: G. Bartoli, M. Bosco, A. Carlone, A. Cavalli, M. Locatelli, A. Mazzanti, P. Ricci, L. Sambri, P. Melchiorre *Angew. Chem. Int. Ed.* **2006**, *45*, 4966.

Table 1 Catalyst study in toluene as solvent^a



Entry	3	solvent	yield (%) ^b	dr ^c	er ^d
1	3a	toluene	91	3:1	64:36
2	3b	Toluene	99	4:1	58:42
2	3c	Toluene	80	4:1	56:44
4	3d	Toluene	99	4:1	52:48
5	3e	Toluene	87	4:1	80:20
7	3f	Toluene	94	4:1	66:34

^aAll reactions run 0.5 M with 0.2 mmol of **1a** and **2a**. ^bYield of isolated product. ^cThe diastereoisomeric ratio was determined by ¹H NMR spectroscopy of the crude reaction mixture. ^dDetermined for the major diastereoisomer by HPLC on a chiral stationary phase.

Table 2 Solvent Study of model reaction with catalyst 3a^a

Entry	Solvent	yield (%) ^b	dr ^c	er ^d
1	CHCl ₃	99	3:1	60:40
2	CH ₃ CN	98	5:1	57:43
3	THF	85	5:1	77:23
4	Et ₂ O	97	4:1	79:21
5	Hexane	99	4:1	66:34
6	C ₆ H ₆	85	3:1	66:34
7	<i>m</i> -xylene	95	4:1	62:38

8 ClC₆H₅ 92 4:1 64:36

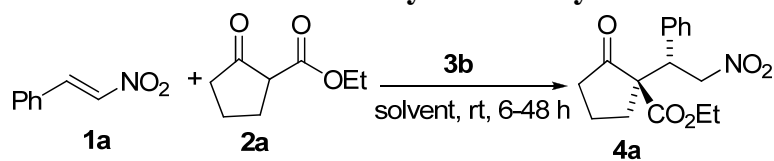
^aAll reactions run 0.5 M with 0.2 mmol of **1a** and **2a**. ^bYield of isolated product. ^cThe diastereoisomeric ratio was determined by ¹H NMR spectroscopy of the crude reaction mixture. ^dDetermined for the major diastereoisomer by HPLC on a chiral stationary phase.

Table 3 Catalysts performance in C₆F₆^a

Entry	3	yield (%) ^b	dr ^c	er ^d
1	3c	94	8:1	85:15
2	3d	98	5:1	52:48
2	3e	64	5:1	77:23
4	3f	70	4:1	59:41

^aAll reactions run 0.5 M with 0.2 mmol of **1a** and **2a**. ^bYield of isolated product. ^cThe diastereoisomeric ratio was determined by ¹H NMR spectroscopy of the crude reaction mixture. ^dDetermined for the major diastereoisomer by HPLC on a chiral stationary phase.

Table 4 Solvent study with catalyst **3b^a**



Entry	3b (mol%)	Solvent	Yield ^b	dr ^c	er ^d
1	15%	Neat	94	5:1	68:32
2 ^e	15%	C ₆ F ₆	98	16:1	85:15
3 ^f	30%	Benzene	97	5:1	73:27

^aAll reactions were carried out with 0.2 mmol of **1a** and **2a**. ^bYield of isolated product. ^cThe diastereoisomeric ratio was determined by ¹H NMR spectroscopy of the crude reaction mixture. ^dDetermined for the major diastereoisomer by HPLC on a chiral stationary phase. ^e Performed at 0 °C at C= 0.2M ^f Performed at C= 0.5M.

Experimental Procedures and Compounds Characterization

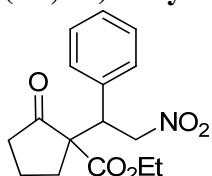
General procedure for synthesis of racemic Michael adducts **4b**, **4d**, **4e**, **4i**, **4k**

In a sample vial β -ketoester **2** (0.2 mmol) was added to a solution of appropriate *trans*-nitroolefin (0.2 mmol) and racemic piperidinemethanol (11.5 mg, 0.1 mmol) in toluene (200 μ L) at room temperature. The mixture was stirred until completion (monitored by TLC, PE/Et₂O 8:2 as eluent), then it was directly loaded onto silica gel and purified by flash chromatography, eluting with PE/Et₂O (8:2 to 7:3) to give racemic adducts (yields from 76 to 97 %).

General procedure for the asymmetric conjugate addition

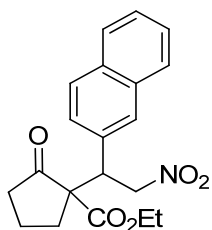
In a sample vial β -ketoester **2** (0.2 mmol) was added to a solution of appropriate *trans*-nitroolefin (0.2 mmol) and catalyst **3b** (10.6 mg, 0.03 mmol) in hexafluorobenzene (500 μ L) at room temperature. The mixture was stirred until completion (monitored by TLC, PE/Et₂O 8:2 as eluent), then it was directly loaded onto silica gel and purified by flash chromatography, eluting with PE/Et₂O (8:2 to 7:3) to give adducts **4a-k**, **5**, **6** and **8**. In case of compound **7**, the reaction was carried out with 10 mol % of catalyst **3b** at C = 0.2 M.

(2*R*, 3*S*)-Ethyl 1-(2-nitro-1-phenylethyl)-2-oxocyclopentanecarboxylate **4a**^{3a}



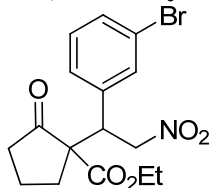
Pale yellow oil; $[\alpha]_D^{20} = -68.1$ (*c* 0.63, CHCl₃); ¹H NMR (CDCl₃, 400 MHz) δ 7.33-7.24 (m, 5H), 5.18 (dd, *J* = 13.6, 4.0 Hz, 1H), 5.01 (dd, *J* = 13.6, 10.8 Hz, 1H), 4.21 (q, *J* = 7.2 Hz, 2H), 4.08 (dd, *J* = 10.8, 4.0 Hz, 1H), 2.41-2.31 (m, 2H), 2.08-1.79 (m, 4H), 1.27 (t, *J* = 7.2 Hz, 3H); ¹³C NMR (CDCl₃, 100 MHz) δ 212.4, 169.3, 135.3, 129.3, 128.8, 128.3, 76.5, 62.4, 62.2, 46.2, 37.9, 31.2, 19.4, 14.0; HPLC analysis with Chiralcel OD-H column, 90:10 *n*-hexane:2-propanol, 0.5 mL/min, detection at 210 nm; minor enantiomer *t*_R = 26.1 min, major enantiomer *t*_R = 36.7 min.

(2*R*, 3*S*)-Ethyl 1-(1-(naphthalen-2-yl)-2-nitroethyl)-2-oxocyclopentanecarboxylate **4b**^{3b}



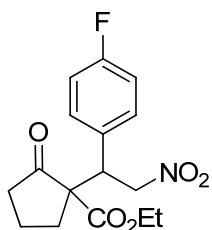
Yellow oil; $[\alpha]_D^{18} = -32.8$ (*c* 1.01, CHCl_3); $^1\text{H NMR}$ (CDCl_3 , 400 MHz) δ 7.81-7.78 (m, 3H), 7.72 (m, 1H), 7.49-7.38 (m, 3H), 5.26 (dd, $J = 13.6, 3.8$ Hz 1H), 5.15 (dd, $J = 13.6, 10.9$ Hz, 1H), 4.27-4.19 (m, 3H), 2.42-2.31 (m, 2H), 2.08-1.96 (m, 2H), 1.94-1.77 (m, 2H), 1.27 (t, $J = 7.2$ Hz, 3H); $^{13}\text{C NMR}$ (CDCl_3 , 100 MHz) δ 212.3, 169.4, 133.1, 132.9, 128.9, 128.7, 128.0, 127.6, 126.7, 126.5, 126.4, 76.6, 62.5, 62.3, 46.3, 37.9, 31.4, 19.4, 14.0; HPLC analysis with Chiralpak IC column, 90:10 *n*-hexane:2-propanol, 1 mL/min, detection at 220 nm; minor enantiomer $t_R = 23.8$ min, major enantiomer $t_R = 31.6$ min.

(2R, 3S)-Ethyl 1-(1-(3-bromophenyl)-2-nitroethyl)-2-oxocyclopentanecarboxylate 4c^{3b}



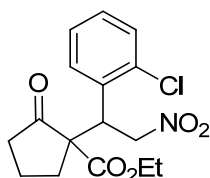
Pale yellow oil; $[\alpha]_D^{18} = -15.9$ (*c* 1.03, CHCl_3); $^1\text{H NMR}$ (CDCl_3 , 400 MHz) δ 7.45-7.42 (m, 2H), 7.28-7.17 (m, 2H), 5.20 (dd, $J = 13.6, 3.6$ Hz, 1H), 5.00 (dd, $J = 14.0, 11.2$ Hz, 1H), 4.21 (q, $J = 7.2$ Hz, 2 H), 3.97 (dd, $J = 10.8, 3.2$ Hz, 1 H), 2.46-2.32 (m, 2 H), 2.17-2.09 (m, 1 H), 1.97-1.67 (m, 3 H), 1.28 (t, $J = 7.2$ Hz, 3 H); $^{13}\text{C NMR}$ (CDCl_3 , 100 MHz) δ 212.1, 169.1, 138.0, 132.3, 131.5, 130.3, 128.1, 122.8, 76.2, 62.3, 62.2, 45.8, 37.8, 31.8, 19.3, 14.0; HPLC analysis with Chiralcel OD-H column, 90:10 *n*-hexane:2-propanol, 0.7 mL/min, detection at 210 nm; minor enantiomer $t_R = 22.9$ min, major enantiomer $t_R = 28.6$ min.

(2R, 3S)-Ethyl 1-(1-(4-fluorophenyl)-2-nitroethyl)-2-oxocyclopentanecarboxylate 4d^{3b}



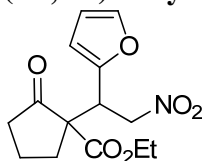
Pale yellow oil; $[\alpha]_D^{19} = -18.6$ (*c* 1.02, CHCl₃); ¹H NMR (CDCl₃, 400 MHz) δ 7.29-7.27 (m, 2H), 7.03-6.98 (m, 2H), 5.15 (dd, *J* = 13.5, 3.8 Hz, 1H), 4.97 (dd, *J* = 13.5, 11.1 Hz, 1H), 4.20 (q, *J* = 7.2 Hz, 2H), 4.05 (dd, *J* = 11.1, 3.6 Hz, 1H), 2.43–2.32 (m, 2H), 2.08-1.82 (m, 4H), 1.27 (t, *J* = 7.2 Hz, 3H); ¹³C NMR (CDCl₃, 100 MHz) δ 212.3, 169.3, 162.4 (d, *J* = 46.5 Hz), 131.2, 131.1, 115.9, 115.7, 77.2, 76.5, 62.4, 62.3, 45.5, 37.9, 31.4, 19.4, 14.0; HPLC analysis with Chiralpak IC column, 80:20 *n*-hexane:2-propanol, 1 mL/min, detection at 220 nm; minor enantiomer *t*_R = 10.2 min, major enantiomer *t*_R = 13.1 min.

(2*R*, 3*S*)-Ethyl 1-(1-(2-chlorophenyl)-2-nitroethyl)-2-oxocyclopentanecarboxylate 4e^{3b}



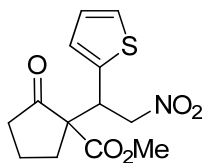
Yellow oil; $[\alpha]_D^{23} = 17.8$ (*c* 0.92, CHCl₃); ¹H NMR (CDCl₃, 400 MHz) δ 7.58-7.55 (m, 1H), 7.40-7.37 (m, 1H), 7.26-7.22 (m, 2H), 5.48 (dd, *J* = 14.1, 3.6 Hz, 1H), 5.10 (dd, *J* = 13.8, 10.5 Hz, 1H), 4.52 (dd, *J* = 10.8, 3.6 Hz, 1H), 4.20 (q, *J* = 7.2 Hz, 2H), 2.49 (t, *J* = 7.5 Hz, 2H), 2.27-1.88 (m, 4H), 1.27 (t, *J* = 7.2 Hz, 3H); ¹³C NMR (CDCl₃, 100 MHz) δ 212.6, 169.3, 135.5, 134.7, 130.1, 129.3, 129.0, 127.6, 76.8, 62.1, 37.8, 33.0, 29.7, 19.3, 14.0; HPLC analysis with Chiralpak IC column, 90:10 *n*-hexane:2-propanol, 1 mL/min, detection at 220 nm; minor enantiomer *t*_R = 19.3 min, major enantiomer *t*_R = 24.5 min.

(2*R*, 3*S*)-Ethyl 1-(1-(furan-2-yl)-2-nitroethyl)-2-oxocyclopentanecarboxylate 4f^{3b}



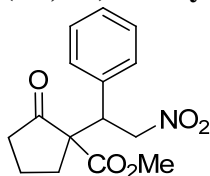
Pale yellow oil; $[\alpha]_D^{23} = -31.4$ (*c* 0.58, CHCl₃); ¹H NMR (CDCl₃, 400 MHz) δ 7.33 (d, *J* = 1.2 Hz, 1H), 6.30 (dd, *J* = 3.3, 1.8 Hz, 1H), 6.18 (d, *J* = 3.2 Hz, 1H), 4.95-4.91 (m, 2H), 4.44 (dd, *J* = 9.8, 4.6 Hz, 1H), 4.21 (q, *J* = 7.2 Hz, 2H), 2.51-2.30 (m, 2H), 2.15-1.95 (m, 3H), 1.80-1.72 (m, 1H), 1.28 (t, *J* = 7.2 Hz, 3H); ¹³C NMR (CDCl₃, 100 MHz) δ 212.1, 168.9, 149.1, 142.7, 110.8, 110.1, 74.5, 62.3, 61.9, 40.4, 37.9, 30.2, 19.5, 14.0; HPLC analysis with Chiralcel OD-H column, 90:10 *n*-hexane:2-propanol, 1 mL/min, detection at 220 nm; minor enantiomer *t*_R = 10.3 min, major enantiomer *t*_R = 14.9 min.

(2*R*, 3*S*)-Methyl 1-(2-nitro-1-(2-thienyl)ethyl)-2-oxocyclopentanecarboxylate 4g^{3c}



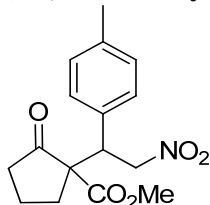
Yellow wax; $[\alpha]_D^{24} = -32.3$ (*c* 0.88, CHCl₃); ¹H NMR (CDCl₃, 400 MHz) δ 7.24-7.23 (m, 1H), 6.96-6.92 (m, 2H), 5.12 (dd, *J* = 13.8, 3.7 Hz, 1H), 4.92 (dd, *J* = 13.8, 10.1 Hz, 1H), 4.41 (dd, *J* = 10.1, 3.7 Hz, 1H), 3.77 (s, 3H), 2.45-2.37 (m, 2H), 2.16-1.91 ppm (m, 4H); ¹³C NMR (CDCl₃, 100 MHz) δ 212.3, 169.8, 137.4, 128.6, 126.8, 126.1, 77.5, 62.4, 53.1, 42.1, 38.0, 31.5, 19.4; HPLC analysis with Chiralcel OD-H column, 88:12 *n*-hexane:EtOH, 0.5 mL/min, detection at 233 nm; minor enantiomer *t*_R = 24.9 min, major enantiomer *t*_R = 42.1 min.

(2*R*, 3*S*)-Methyl 1-(2-nitro-1-phenylethyl)-2-oxocyclopentanecarboxylate 4h^{3c}



White wax; $[\alpha]_D^{20} = -24.3$ (*c* 1.00, CHCl₃); ¹H NMR (CDCl₃, 400 MHz) δ 7.32-7.22 (m, 5H), 5.20-5.14 (dd, *J* = 13.8, 4.2 Hz, 1H), 5.07-4.98 (dd, *J* = 13.5, 10.8 Hz, 1H), 4.08 (dd, *J* = 10.8, 3.9 Hz, 1H), 3.76 (m, 3H), 2.30-2.43 (m, 2H), 1.77-2.09 (m, 4H); ¹³C NMR (CDCl₃, 100 MHz) δ 212.2, 169.8, 135.2, 129.3, 128.8, 128.3, 76.4, 62.4, 53.1, 46.2, 37.9, 31.1, 19.3; HPLC analysis with Chiralcel OD-H column, 90:10 *n*-hexane:2-propanol, 1 mL/min, detection at 220 nm; minor enantiomer *t*_R = 17.0 min, major enantiomer *t*_R = 25.2 min.

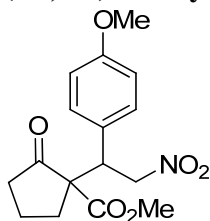
(2*R*, 3*S*)-Methyl 1-(2-nitro-1-*p*-tolylethyl)-2-oxocyclopentanecarboxylate 4i^{3d}



Pale yellow oil; $[\alpha]_D^{24} = -24.2$ (*c* 0.97, CHCl₃); ¹H NMR (CDCl₃, 400 MHz) δ 7.14-7.08 (m, 4H), 5.13 (dd, *J* = 13.2, 4.5 Hz, 1H), 4.99 (dd, *J* = 13.2, 11.1 Hz, 1H), 4.07 (dd, *J* = 10.8, 3.6 Hz, 1H), 3.76 (s, 3H), 2.52-2.34 (m, 2H), 2.30 (s, 3H), 2.07-1.77 (m, 4H); ¹³C NMR (CDCl₃, 100 MHz) δ 212.64, 170.07, 138.36, 132.20, 129.78, 129.35, 76.68, 62.74, 53.31, 46.03, 38.26, 31.18, 21.29, 19.61; HPLC

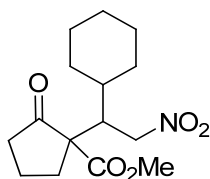
analysis with Chiralpak IC column, 90:10 *n*-hexane:2-propanol, 1 mL/min, detection at 220 nm; minor enantiomer $t_R = 22.5$ min, major enantiomer $t_R = 33.6$ min.

(2*R*, 3*S*)-Methyl 1-(1-(4-methoxyphenyl)-2-nitroethyl)-2-oxocyclopentanecarboxylate 4j^{3d}



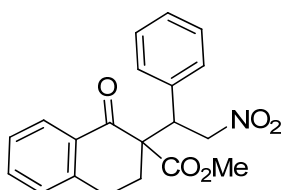
Pale yellow oil; ¹H NMR (CDCl₃, 400 MHz) 7.18–7.15 (m, 2H), 6.84–6.82 (m, 2H), 5.11 (dd, *J* = 13.3, 4.1 Hz, 1 H), 4.89–5.01 (dd, *J* = 13.3, 11 Hz, 1H), 4.04 (dd, *J* = 11.0, 4.1 Hz, 1H), 3.78 (s, 3H), 3.75 (s, 3H), 2.44–2.30 (m, 2H), 2.06–1.80 (m, 4H); ¹³C NMR (CDCl₃, 100 MHz) δ 212.3, 169.8, 159.3, 130.4, 126.9, 114.1, 76.5, 62.6, 55.1, 53.0, 45.4, 37.9, 30.9, 19.3; HPLC analysis with Chiralpak ASH column, 90:10 *n*-hexane:2-propanol, 1 mL/min, detection at 220 nm; minor enantiomer $t_R = 31.5$ min, major enantiomer $t_R = 24.8$ min.

(2*R*, 3*S*)-Methyl 1-(1-cyclohexyl-2-nitroethyl)-2-oxocyclopentanecarboxylate 4k^{3d}



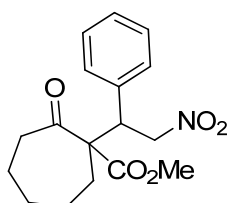
Pale yellow oil; $[\alpha]_D^{24} = -34.1$ (*c* 0.33, CHCl₃); ¹H NMR (CDCl₃, 400 MHz) δ 5.06 (dd, *J* = 15.6, 3.9 Hz, 1H), 4.53 (dd, *J* = 14.7, 5.7 Hz, 1H), 3.66 (s, 3H), 2.73–2.64 (m, 2H), 2.42–2.37 (m, 2H), 2.01–2.00 (m, 3H), 1.70–1.47 (m, 5H), 1.20–0.98 (m, 6H); ¹³C NMR (CDCl₃, 100 MHz) δ 213.18, 170.18, 74.01, 62.29, 52.98, 45.30, 39.54, 38.10, 33.00, 32.40, 28.80, 27.02, 26.73, 26.10, 19.48; HPLC analysis with Chiralpak IC column, 97:3 *n*-hexane:2-propanol, 1 mL/min, detection at 220 nm; minor enantiomer $t_R = 38.9$ min, major enantiomer $t_R = 47.8$ min.

Methyl 2-(2-nitro-1-phenylethyl)-1-oxo-1,2,3,4-tetrahydronaphthalene-2-carboxylate 5^{3d}



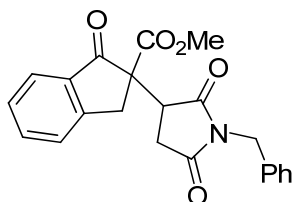
White solid; ^1H NMR (CDCl_3 , 400 MHz) (*major diastereoisomer*) δ 8.05 (d, $J = 8.1$ Hz, 1H), 7.52 (t, $J = 7.2$ Hz, 1H), 7.38-7.28 (m, 6H), 7.20 (d, $J = 7.5$ Hz, 1H), 5.16 (dd, $J = 13.8, 4.5$ Hz, 1H), 5.06 (dd, $J = 13.2, 10.2$ Hz, 1H), 4.21 (dd, $J = 10.2, 3.6$ Hz, 1H), 3.65 (s, 3H), 2.99-2.95 (m, 2H), 2.46-2.32 (m, 1H), 2.08-1.99 (m, 1H); ^{13}C NMR (CDCl_3 , 100 MHz) δ 194.45, 170.48, 142.72, 136.10, 134.34, 130.08, 129.59, 128.98, 128.89, 128.68, 128.50, 127.32, 78.09, 59.95, 53.02, 47.35, 30.99, 25.77; HPLC analysis with Chiralcel OD column, 90:10 *n*-hexane:2-propanol, 1 mL/min, detection at 254 nm; major diastereoisomer [$t_R = 35.6$ min (minor enantiomer), $t_R = 19.4$ min (major enantiomer)]; minor diastereoisomer [$t_R = 24.5$ min (minor enantiomer), $t_R = 51.0$ min (major enantiomer)].

(2*R*, 3*S*)- Methyl 1-(2-nitro-1-phenylethyl)-2-oxocycloheptanecarboxylate 6^{3a}



Colorless oil; ^1H NMR (CDCl_3 , 400 MHz) (*major diastereoisomer*) δ 7.35-7.25 (m, 3H), 7.21-7.10 (m, 2H), 5.00-4.89 (m, 2H), 4.07 (dd, $J = 10.1, 4.3$ Hz, 1H), 3.78 (s, 3H), 2.66-2.49 (m, 2H), 2.53 (ddd, $J = 12.7, 8.9, 4.3$ Hz, 1H), 1.94-1.40 (m, 8H); ^{13}C NMR (CDCl_3 , 100 MHz) δ 208.3, 171.3, 135.5, 129.4, 128.7, 128.3, 77.8, 65.4, 52.4, 48.4, 41.3, 32.8, 28.9, 25.0, 24.4; HPLC analysis with Chiralcel OD-H column, 95:5 *n*-hexane:2-propanol, 1 mL/min, detection at 220 nm; major diastereoisomer [$t_R = 14.3$ min (minor enantiomer), $t_R = 31.3$ min (major enantiomer)], minor diastereoisomer [$t_R = 13.1$ min (minor enantiomer), $t_R = 27.2$ min (major enantiomer)].

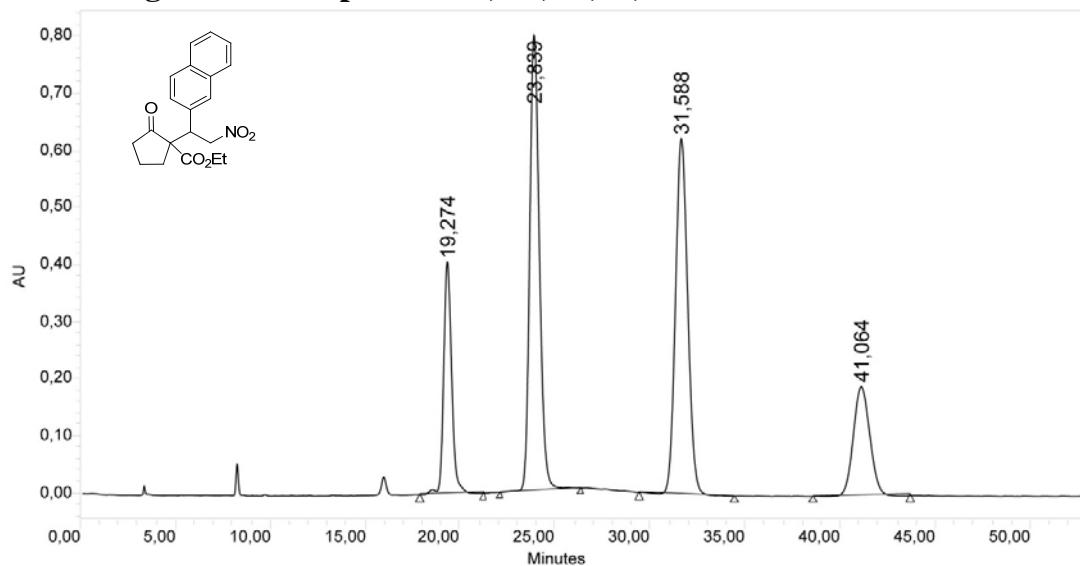
Methyl 2-(3-benzyl-2,4-dioxocyclopentyl)-1-oxo-2,3-dihydro-1H-indene-2-carboxylate 8^{3e}



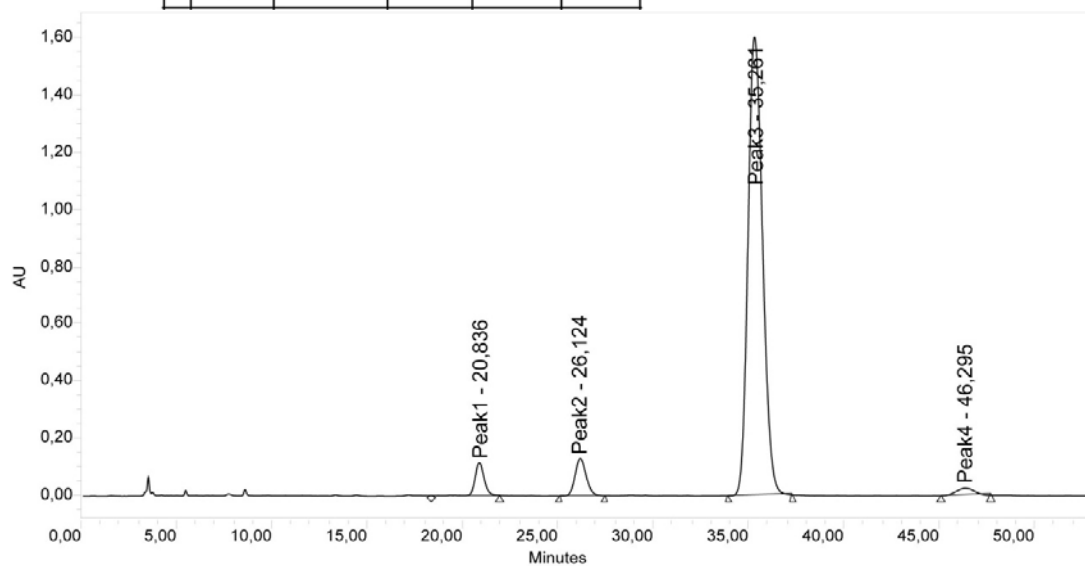
White solid; ^1H NMR (CDCl_3 , 400 MHz) (*1/1 mixture of diastereoisomers*) δ 7.72-7.69 (m, 1H), 7.66-7.61 (m, 1.8H), 7.50-7.32 (m, 3.7H), 7.30-7.25 (m, 9.3H), 4.60 (m, 3.8H), 4.06 (dd, $J = 9.2, 6.0$ Hz, 1H), 4.05-3.95 (m, 0.9H), 3.75 (s, 2.5H), 3.28-3.02 (m, 1.8H), 3.0-2.78 (m, 1.9H), 2.38 (dd, $J = 18.4, 6.0$ Hz, 1H), 2.35-2.19 (m, 0.9H); ^{13}C NMR (CDCl_3 , 100 MHz) δ 200.2, 199.5, 176.9, 176.6, 175.6,

174.9, 170.2, 169.2, 152.8, 152.4, 136.1, 135.8, 135.4, 134.7, 134.6, 128.7, 128.6, 128.5, 128.2, 127.9, 127.8, 126.4, 124.9, 60.5, 60.7, 53.4, 53.0, 43.9, 43.1, 42.5, 37.1, 34.0, 32.3, 31.4, 26.3; HPLC analysis with Chiralpak AD-H column, 75:25 *n*-hexane:2-propanol, 0.75 mL/min, detection at 254 nm; major diastereoisomer [$t_R = 27.0$ min (minor enantiomer), $t_R = 34.8$ min (major enantiomer)], minor diastereoisomer [$t_R = 36.4$ min (minor enantiomer), $t_R = 22.4$ min (major enantiomer)].

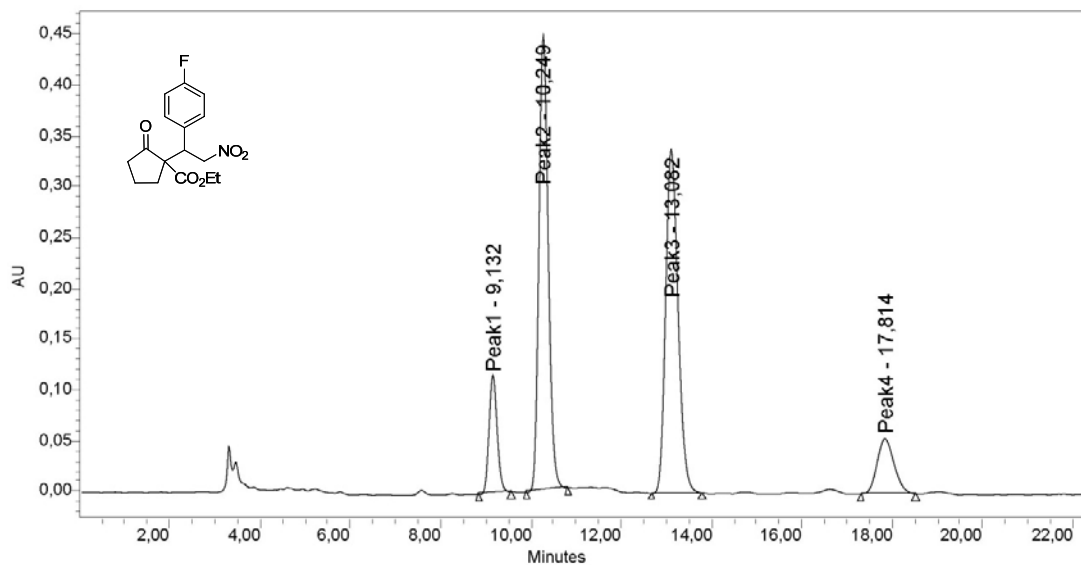
HPLC chromatograms of compounds 4b, 4d, 4e, 4i, 4k



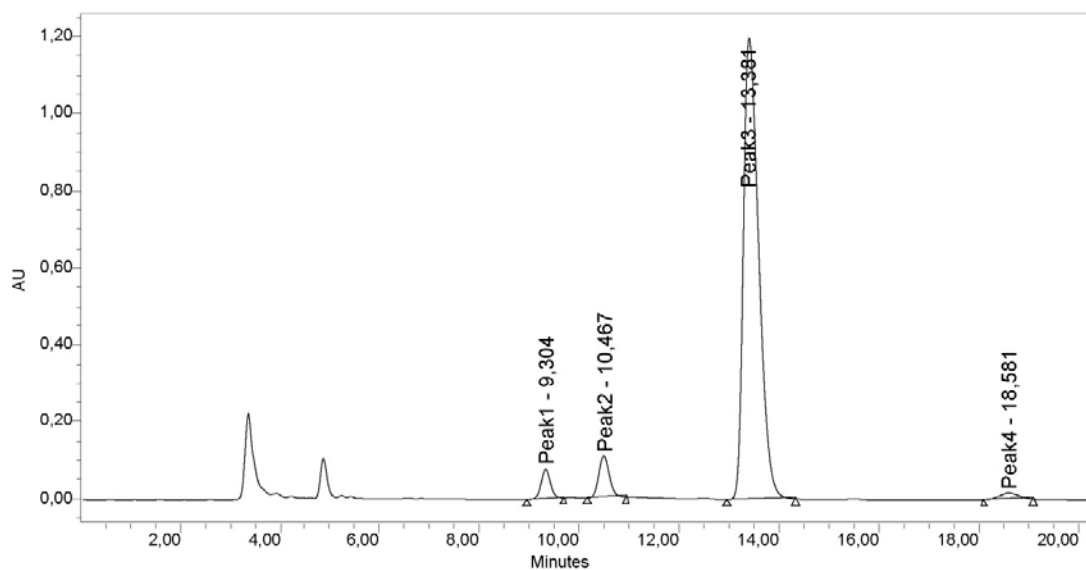
	RT (min)	Area (V*sec)	% Area	Height (V)	% Height
1	19,274	11962356	15,03	406304	20,13
2	23,839	28205558	35,44	797707	39,52
3	31,588	27845789	34,98	622979	30,87
4	41,064	11581654	14,55	191283	9,48



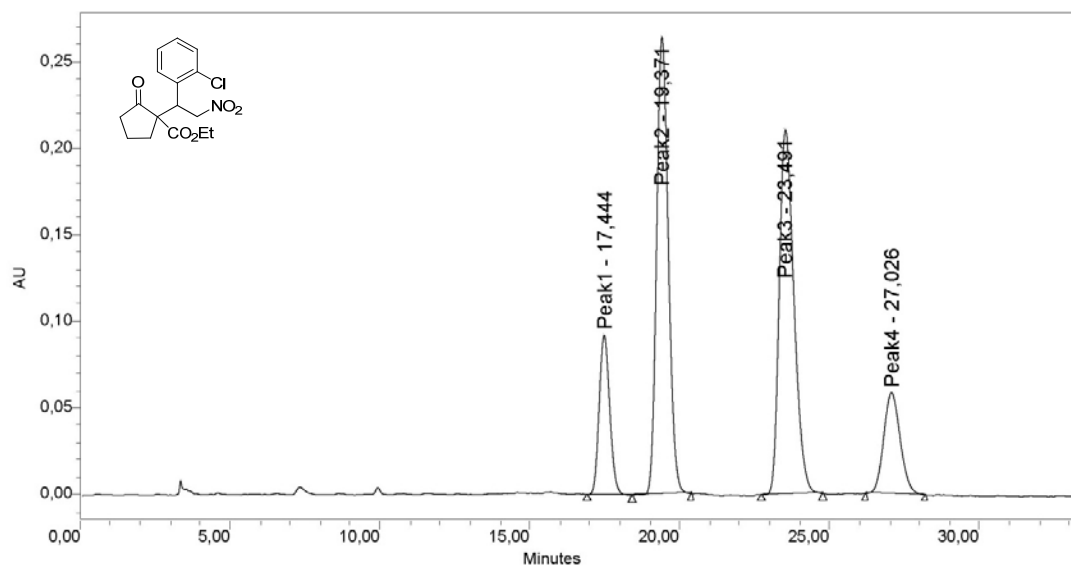
	Peak Name	RT (min)	Area (V*sec)	% Area	Height (V)	% Height
1	Peak1	20,836	3842164	4,00	114940	6,13
2	Peak2	26,124	5282882	5,49	129861	6,92
3	Peak3	35,261	85320554	88,74	1605121	85,59
4	Peak4	46,295	1704128	1,77	25514	1,36



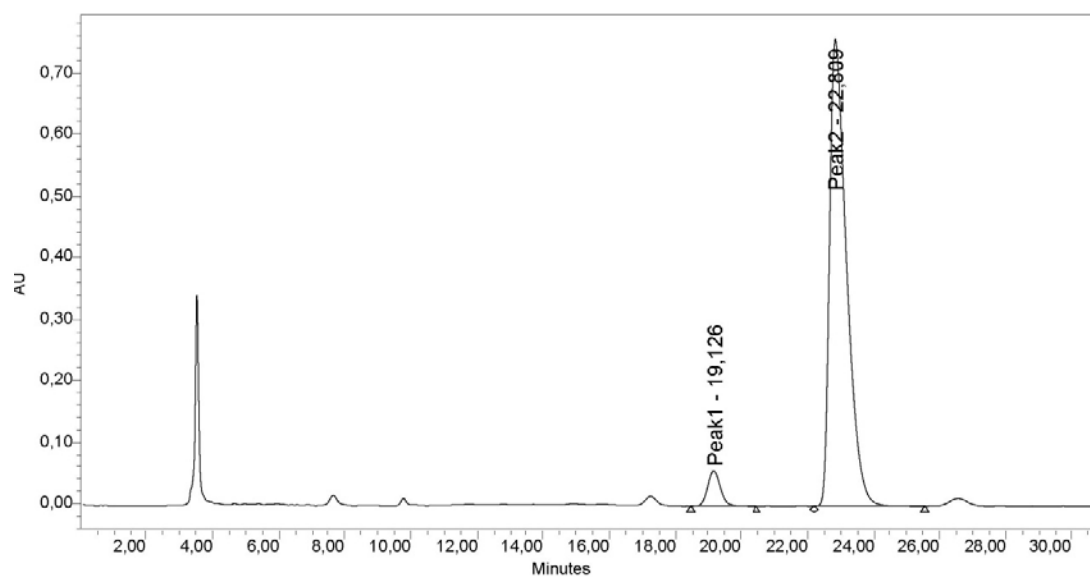
Peak Name	RT (min)	Area (V*sec)	% Area	Height (V)	% Height
1 Peak1	9,132	1463260	9,29	116819	12,19
2 Peak2	10,249	6417742	40,73	448362	46,77
3 Peak3	13,082	6451955	40,95	338953	35,36
4 Peak4	17,814	1424320	9,04	54453	5,68



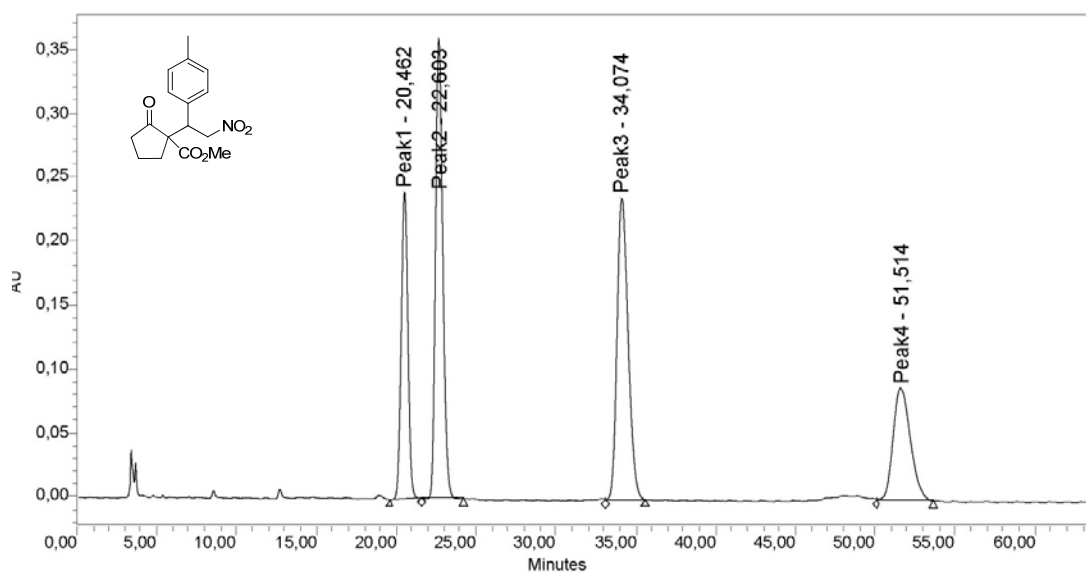
Peak Name	RT (min)	Area (V*sec)	% Area	Height (V)	% Height
1 Peak1	9,304	980353	3,44	76844	5,49
2 Peak2	10,467	1594090	5,59	108173	7,73
3 Peak3	13,381	25537109	89,51	1198387	85,61
4 Peak4	18,581	419020	1,47	16409	1,17



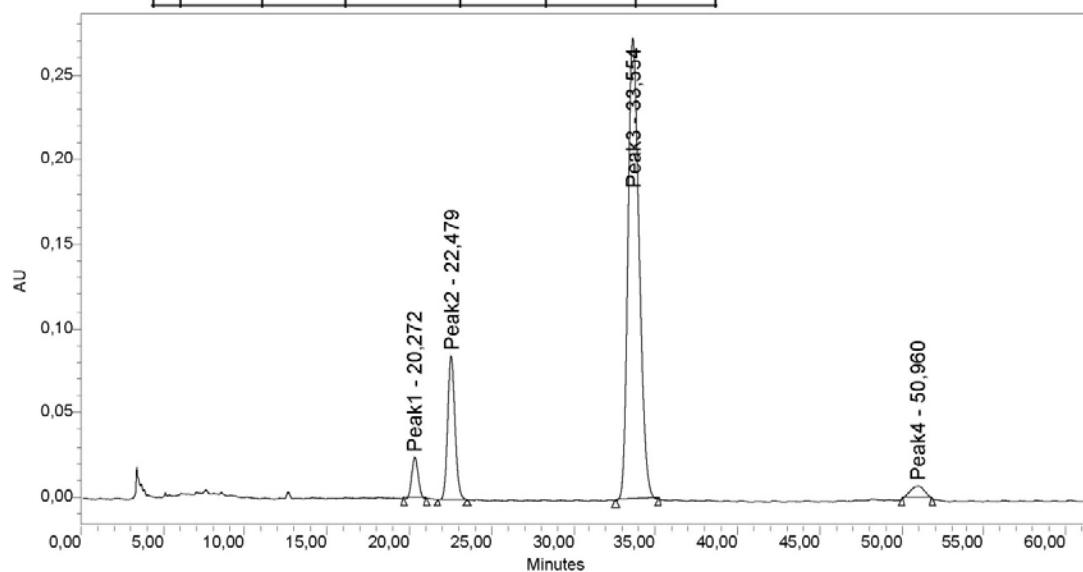
Peak Name	RT (min)	Area (UV*sec)	% Area	Height (UV)	% Height
1 Peak1	17,444	2269676	12,02	92448	14,76
2 Peak2	19,371	7177954	38,03	264306	42,20
3 Peak3	23,491	7169053	37,98	210894	33,67
4 Peak4	27,026	2258923	11,97	58717	9,37



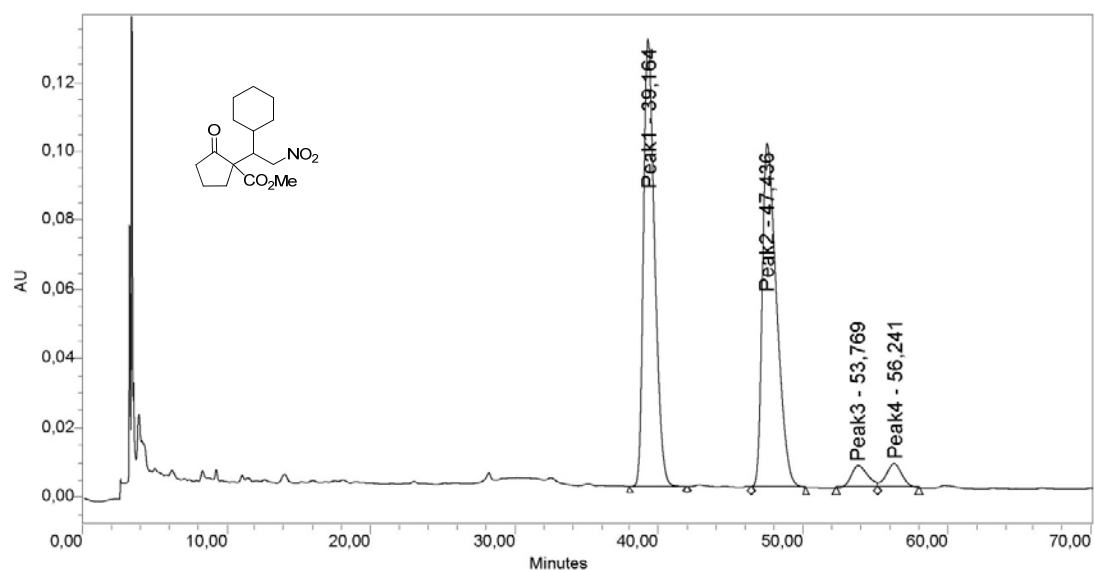
Peak Name	RT (min)	Area (UV*sec)	% Area	Height (UV)	% Height
1 Peak1	19,126	1548335	5,41	57272	7,02
2 Peak2	22,809	27079411	94,59	758563	92,98



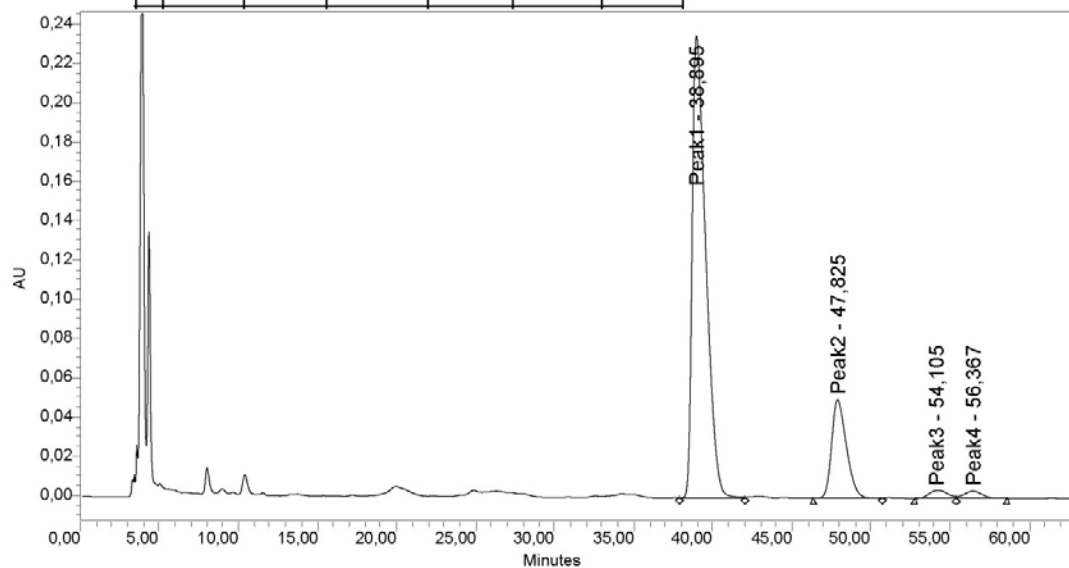
Peak Name	RT (min)	Area (UV*sec)	% Area	Height (UV)	% Height
1 Peak1	20,462	7058649	19,20	240835	25,99
2 Peak2	22,603	11464924	31,19	360437	38,89
3 Peak3	34,074	11460798	31,17	236488	25,52
4 Peak4	51,514	6778540	18,44	88970	9,60



Peak Name	RT (min)	Area (UV*sec)	% Area	Height (UV)	% Height
1 Peak1	20,272	686697	4,09	24899	6,36
2 Peak2	22,479	2647444	15,78	85437	21,84
3 Peak3	33,554	12991382	77,43	273543	69,92
4 Peak4	50,960	452991	2,70	7369	1,88



Peak Name	RT (min)	Area (ΔV*sec)	% Area	Height (ΔV)	% Height
1 Peak1	39,164	6964025	46,52	129406	53,36
2 Peak2	47,436	6931609	46,31	99576	41,06
3 Peak3	53,769	531868	3,55	6441	2,66
4 Peak4	56,241	541639	3,62	7075	2,92



Peak Name	RT (min)	Area (ΔV*sec)	% Area	Height (ΔV)	% Height
1 Peak1	38,895	13986402	78,45	235004	80,33
2 Peak2	47,825	3224056	18,08	49899	17,06
3 Peak3	54,105	329157	1,85	3955	1,35
4 Peak4	56,367	287862	1,61	3675	1,26

Computational Details

The DFT geometry optimizations were performed at the GGA level with the Gaussian09 package,⁴ using the BP86 functional of Becke and Perdew.⁵ The electronic configuration of the molecular systems was described with the standard split-valence plus basis set with a polarization function of Ahlrichs and co-workers (SVP keyword in Gaussian09).⁶ The geometry optimizations were performed without symmetry constraints, and the characterization of the located stationary points was performed by analytical frequency calculations. The energies discussed in the text have been obtained through single point energy calculations on the BP86/SVP optimized geometries using the M06 functional⁷ in connection with the TZVP basis set.⁸ Solvent effects including contributions of non electrostatic terms have been estimated in single point calculations on the gas phase optimized structures, based on the polarizable continuous solvation model PCM, using toluene or C₆F₆ as the solvent.⁹ Zero point energy and thermal corrections were included from gas-phase vibrational analysis at the BP86 level on the SVP optimized geometries.

Gas-phase BP86/TZVP energy of the calculated transition states

Table S1. Relative free energy, in kcal/mol, of the four possible transition states for the reaction of **1a** and **2a** promoted by **3a**. Geometries have been optimized in the gas-phase with the BP86 functional

⁴ **Gaussian 09, Revision A.1**, M. J. Frisch, G. W. Trucks, H. B. Schlegel, G. E. Scuseria, M. A. Robb, J. R. Cheeseman, G. Scalmani, V. Barone, B. Mennucci, G. A. Petersson, H. Nakatsuji, M. Caricato, X. Li, H. P. Hratchian, A. F. Izmaylov, J. Bloino, G. Zheng, J. L. Sonnenberg, M. Hada, M. Ehara, K. Toyota, R. Fukuda, J. Hasegawa, M. Ishida, T. Nakajima, Y. Honda, O. Kitao, H. Nakai, T. Vreven, J. A. Montgomery, Jr., J. E. Peralta, F. Ogliaro, M. Bearpark, J. J. Heyd, E. Brothers, K. N. Kudin, V. N. Staroverov, R. Kobayashi, J. Normand, K. Raghavachari, A. Rendell, J. C. Burant, S. S. Iyengar, J. Tomasi, M. Cossi, N. Rega, J. M. Millam, M. Klene, J. E. Knox, J. B. Cross, V. Bakken, C. Adamo, J. Jaramillo, R. Gomperts, R. E. Stratmann, O. Yazyev, A. J. Austin, R. Cammi, C. Pomelli, J. W. Ochterski, R. L. Martin, K. Morokuma, V. G. Zakrzewski, G. A. Voth, P. Salvador, J. J. Dannenberg, S. Dapprich, A. D. Daniels, Ö. Farkas, J. B. Foresman, J. V. Ortiz, J. Cioslowski and D. J. Fox, Gaussian, Inc., Wallingford CT, **2009**.

⁵ (a) A. D. Becke, *Phys. Rev. A*, **1988**, 38, 3098, (b) J. P. Perdew, *Phys. Rev. B*, **1986**, 33, 8822., (c) J. P. Perdew, *Phys. Rev. B*, **1986**, 34, 7406.

⁶ A. Schaefer, H. Horn and R. Ahlrichs, *J. Chem. Phys.*, **1992**, 97, 2571.

⁷ Y. Zhao; D. G. Truhlar, *Theor Chem Acc.*, **2008**, 120, 215.

⁸ A. Schaefer; C. Huber; R. Ahlrichs, *J. Chem. Phys.*, **1994**, 100, 5829.

⁹ V. Barone and M. Cossi, *J. Phys. Chem. A*, **1998**, 102, 1995.

and the SVP basis set. The energy of the structures in bold has been further refined through single point energy calculations in solvent with the M06 functional and the TZVP basis set.

	E (kcal/mol)
Pro-S,R	0.0
Pro-R,S	0.4
Pro-R,R	1.6
Pro-S,S	0.6
Pro-S,R +C₆F₆	0.0
Pro-R,S +C₆F₆	1.3
Pro-S,R +2C ₆ F ₆	0.0
Pro-R,S +2C ₆ F ₆	1.3

#

BP86 and M06 interaction energy between the C₆F₆ molecule and the reacting system in transition state pro-S,R +C₆F₆.

The interaction energy between the reacting system and the C₆F₆ molecule in transition state pro-S,R +C₆F₆ is calculated as follows:

$$E(\text{interaction}) = -[E(\text{pro-S,R} + \text{C}_6\text{F}_6) - E(\text{pro-S,R}) - E(\text{C}_6\text{F}_6)]$$

With this approach, $E(\text{interaction})$ is calculated to be 4.8 kcal/mol in the gas-phase at the BP86/SVP level, and 14.6 kcal/mol in solvent at the M06/TZVP level. Although the BP86 value can be affected by the BSSE, the strong interaction at the M06 level indicates a rather strong interaction more driven by electrostatic interaction rather than dispersion. This strong interaction is more typical of a well defined minimum on the potential energy surface, rather than of a rather floppy potential energy surface.

Steric profiles in transition states pro-R,S and pro-S,R

The closer proximity between C₆F₆ and the enolate in TS pro-R,S can be rationalized by visual inspection of the steric profiles of the TS, see Figure S1.

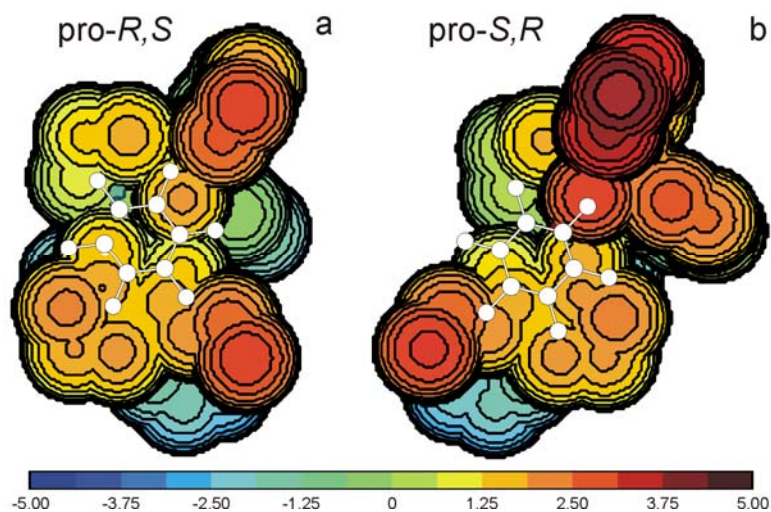


Figure S1. Steric profile of the pro-*R,S* and pro-*S,R* TS. The optimized geometry of C₆F₆, in white, is plotted on top of the steric profiles.

In case of TS pro-*R,S*, steric hindrance by one of the Ph rings of the catalyst and the ethoxy group of **2a** is higher on the right side, as evidenced by the red isocontour lines. On the left side, instead, the orange isocontour lines indicates reduced steric hindrance, so that C₆F₆ can be accommodated comfortably above the enolate. Differently, in TS pro-*S,R* the ethoxy group is placed on the left of the catalyst, see Figures 1b and 2b, so that the ethoxy group and one of the Ph rings of the catalyst shape a narrow groove preventing optimal stacking of C₆F₆ on top of the enolate.

The steric profiles of Figure S1 have been calculated using the geometry of transition states pro-*R,S* and pro-*S,R* in presence of a C₆F₆ molecule. The points in space defining the steric profile were located with the SambVca package developed by us.¹⁰ This program is normally used to calculate the buried volume of a given ligand, which is a number that quantifies the amount of the first coordination sphere of the metal occupied by this ligand.¹¹ We modified SambVca to understand the disposition and the steric hindrance of the reactants and of the catalyst in the reactive pocket. We already introduced topographic steric profiles in the context of Rh- and Ru- catalysis.¹²

¹⁰ A. Poater, B. Cosenza, A. Correa, S. Giudice, F. Ragone, V. Scarano, L. Cavallo, *Eur. J. Inorg. Chem.* **2009**, 1759.

¹¹ (a) L. Cavallo, A. Correa, C. Costabile, H. Jacobsen, *J. Organomet. Chem.* **2005**, 690, 5407, (b) A. Poater, F. Ragone, S. Giudice, C. Costabile, R. Dorta, S. P. Nolan, L. Cavallo, *Organometallics* **2008**, 27, 2679, (c) A. C. Hillier, W. J. Sommer, B. S. Yong, J. L. Petersen, L. Cavallo, S. P. Nolan, *Organometallics* **2003**, 22, 4322.

¹² (a) A. Poater, F. Ragone, R. Mariz, R. Dorta, L. Cavallo, *Chem. Eur. J.* **2010**, 16, 14348, (b) F. Ragone, A. Poater, L. Cavallo, *J. Am. Chem. Soc.* **2010**, 132, 4249.

To build the steric profile, the geometry of transition states pro-*R,S* and pro-*S,R* has been placed with the C2 atom at the origin, with the C2-C3 bond aligned along the z-axis at negative z values, and with the C3 C4 bond in the yz plane at positive y values. After this alignment step a sphere centered around the C2 atom is analyzed. This sphere, of radius *R*, is sectioned by a regular 3D cubic mesh of spacing *s*, which defines cubic voxels *v*. The distance between the centre of each voxel with all the atoms in the ligand is tested to check if any of the atoms is within a van der Waals distance from the centre of the examined voxel. If no atom is within a van der Waals distance, the examined voxel is marked as a free voxel. Otherwise, the examined voxel is marked as buried.

After all the voxels in the sphere have been marked as free or buried, for each (x,y) point within the sphere the program scans the sphere from the bottom (i.e. at negative z values) to find at which z value there is the first buried voxel. This procedure results in a surface, defined as $S(x,y) = z_B$, which represents the VdW surface of the atoms in the considered geometry. In other words, this $S(x,y) = z_B$ surface defines the shape of the reactive pocket.

Finally, the maps are a simple 2D isocontour representation of the interaction surface $S(x,y) = z_B$. In this work, the radius *R* of the sphere around the metal center was set to 15 Å, while for the atoms we adopted the Bondi radii¹³ scaled by 1.17, and a mesh of 0.1 Å was used to scan the sphere for buried voxels.

¹³ A. Bondi, J. Phys. Chem. 1964, 68, 441.

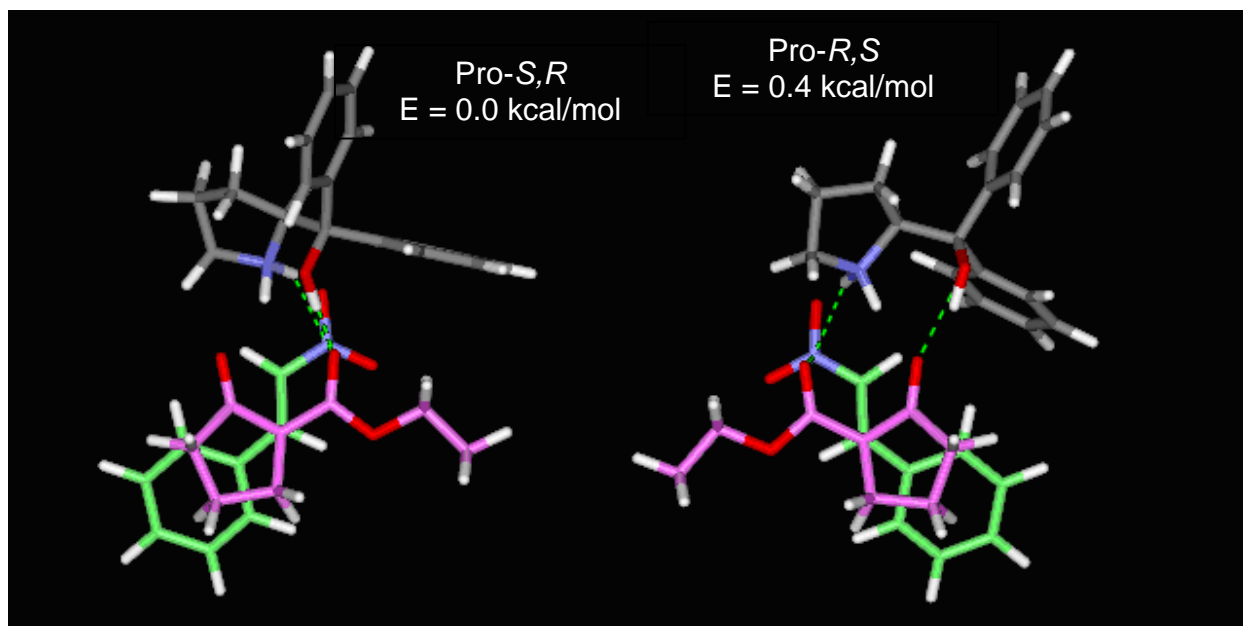


Figure S2. Structure of the pro-*S,S* and pro-*R,R* transition states and their relative energy with respect to the pro-*S,R* transition state. Structures are oriented along the forming C2-C3 bond. C atoms of **1a** and **2a** are colored in pale green and pink, respectively.

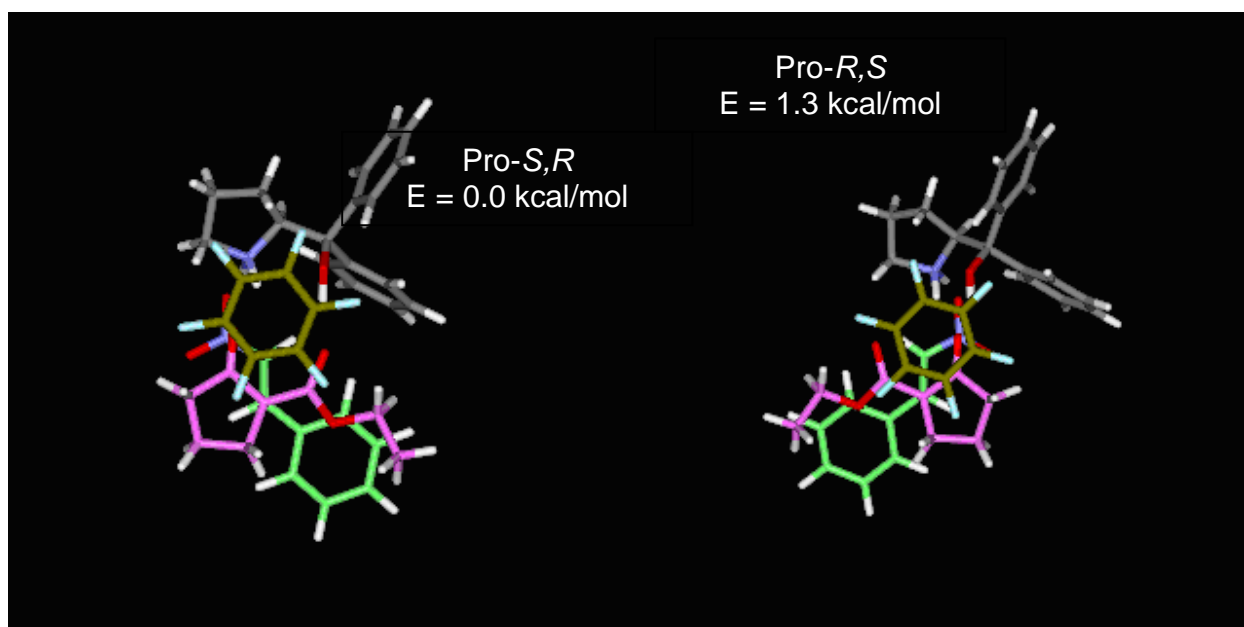


Figure S3. Structure of the pro-*S,R* and pro-*R,S* transition states in presence of a C₆F₆ molecule. Structures are oriented along the forming C2-C3 bond. C atoms of **1a** and **2a** are colored in pale green and pink, respectively. C and F atoms of C₆F₆ are colored in olive green and light blue, respectively.

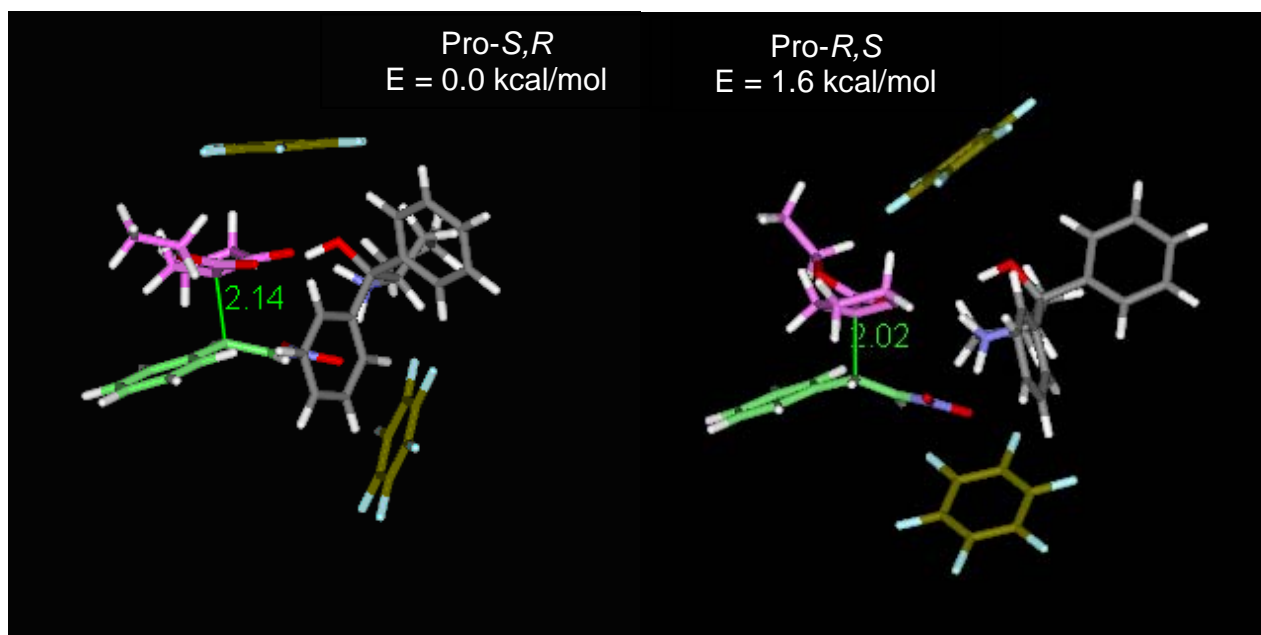


Figure S4. Structure of the pro-*S,R* and pro-*R,S* transition states in presence of 2 C₆F₆ molecules. Structures are oriented along the forming C2-C3 bond. C atoms of **1a** and **2a** are colored in pale green and pink, respectively. C and F atoms of C₆F₆ are colored in olive green and light blue, respectively.

pro- <i>S,R</i> +C ₆ F ₆ -2666.8378078a.u.	pro- <i>R,S</i> +C ₆ F ₆ -2666.8355536a.u.	pro- <i>S,R</i> +2C ₆ F ₆ -3493.8499269a.u.	pro- <i>R,S</i> +2C ₆ F ₆ -3493.846668a.u.		
O 0.443698	1.530287	1.490240	O 0.733004	0.683744	0.943177
C 1.600780	1.548681	1.331911	C 0.467664	1.710614	1.703655
C 2.451259	2.631152	2.073557	C 0.887324	1.908902	3.500200
C 3.920101	2.395495	1.678336	C 0.171400	3.205255	3.487435
C 3.844854	1.681857	0.305004	C -0.103880	3.991859	2.174950
C 2.557892	0.865935	0.377440	C -0.207753	2.922832	1.089518
H 2.075770	3.613161	1.708074	H 1.997248	2.016635	3.045226
H 2.242483	2.584642	3.160192	H 0.662792	1.000417	3.649435
H 4.406781	1.736554	2.283600	H -0.787480	2.966044	3.996578
H 4.517425	3.328554	1.636795	H 0.762052	3.797070	4.212151
H 3.767179	2.425547	-0.519863	H 0.708921	4.709609	1.940499
H 4.739654	1.065762	0.077451	H -1.025313	4.614544	2.249150
C 1.953984	0.304443	-0.840811	C 0.131960	3.225549	-0.327475
O 0.847770	-0.245679	-0.931426	O 0.113449	2.409055	-1.249304
O 2.769085	0.430313	-1.920241	O 0.497691	4.522554	-0.497455
C 2.265154	-0.076359	-3.178688	C 0.920037	5.412136	-1.825645
H 2.013437	-0.151423	-3.057172	H -0.000780	1.914049	-2.420939
H 1.322460	0.456876	-3.424488	H 1.436257	4.054504	-2.292711
N 1.414999	-1.073979	3.175109	N -2.281910	3.529681	1.022390
O 1.992758	-0.185450	3.840482	O -2.066414	0.005817	2.253517
O 0.320122	-1.624594	3.628577	O -2.397201	-1.076784	0.335188
C 1.902047	-1.511516	1.961437	C -2.396485	4.226662	0.328778
H 1.316894	-2.308477	1.490554	H -2.714011	1.139543	-0.716594
C 3.065192	-0.913625	1.416364	C -1.269105	2.463372	0.993748
H 3.643641	-0.350985	2.166646	H -2.253836	2.379647	2.087651
C 3.894589	-1.657365	0.431020	C -2.282825	3.681137	0.431909
C 5.557577	-1.301583	-1.366974	C -4.195191	5.955932	-0.592514
C 5.503762	-1.516419	0.463145	C -3.513646	4.563344	1.297247
C 3.352227	-2.542590	-0.524343	C -2.831477	3.965470	-0.952040
C 4.158820	-3.255331	-1.404833	C -3.212161	5.086534	-1.456938
C 6.127184	-2.229996	-0.420516	C -4.191823	5.690899	0.792410
H 5.758516	-0.854748	1.221052	H -3.527200	4.357580	2.238136
H 2.243628	-2.672143	-0.587155	H -2.286278	3.299224	-1.637196
H 3.703571	-3.943609	-2.138679	H -3.499081	5.289533	-2.538332
H 7.220983	-2.109012	-0.367831	H -4.724585	6.359952	1.487846
H 6.200834	-3.665919	-2.057946	H -4.736469	6.328411	-0.999862
N -1.494097	-0.352836	2.262353	N -0.161380	-0.885565	-1.085046
C -1.970543	0.685218	3.258464	C 0.597004	2.216536	-1.088179
C -3.505911	0.623033	1.397417	C 1.255841	-2.184928	-2.478340
C -3.789570	0.065960	1.792268	C 0.876630	-1.675876	-3.321588
C -2.689810	-0.996016	1.611018	C -0.284463	-0.425934	-2.531948
H -1.563461	1.659611	2.931143	H -0.176754	-3.009443	-1.094264
H -1.532140	0.441969	4.245119	H 1.705038	-3.141913	-2.799155
H -3.900646	-0.068309	3.972359	H 2.061018	-1.414968	-2.453875
H -3.966418	1.615413	3.317786	H 0.260906	-1.515051	-4.401610
H -3.669732	0.853883	1.020049	H -0.765476	-2.396927	-3.222316
H -4.803358	-0.363262	1.683486	H 0.304756	-0.121516	-0.522088
H -2.952913	-1.893611	2.282625	H -1.123552	-0.932654	-0.573556
H -0.894494	0.148750	1.555385	C 1.818608	6.151436	-1.703565
C -2.384504	-1.409243	0.130548	H 1.700552	6.617129	-0.705142
C -3.735931	-1.751173	-0.540912	H 5.592790	6.921776	-2.458018
C -6.222470	-3.361977	-1.746752	H 2.288800	5.891972	-1.833462
C -4.492970	-2.860950	-0.104770	C 1.532636	-2.420498	0.157349
C -4.232781	-0.957199	-1.592216	H -1.285541	-0.007357	-2.719696
C -5.468489	-1.263481	-2.191277	O 0.463546	0.376014	-2.669725
C -5.728830	-3.161950	-0.699706	O 2.375337	-1.283233	0.284684
H -4.104458	-3.513498	0.964272	H 1.812049	-0.576355	0.709876
H -3.683730	-0.098403	-1.932310	C 2.444907	-3.636171	-0.138366
H -5.843227	-0.634199	-0.314731	C 3.082325	-4.960392	0.183259
H -6.305137	-4.033568	-0.350977	C 2.673273	-3.409387	-0.784279
H -7.189507	-2.600417	-2.217660	C 1.920817	-6.037662	-0.152475
H -1.468082	-2.645695	-0.003123	H 1.123638	-5.152445	0.706204
C 0.123535	-4.953964	-0.445739	C 4.522960	-4.484126	-1.104779
C -1.075934	-3.467861	1.072623	H 3.980495	-2.371195	-0.995145
C -1.046096	-2.998125	-1.307818	C 1.354445	-5.800979	-0.792798
C -0.259687	-4.137274	-1.527157	H 5.296331	-7.064276	0.104271
C -0.283867	-4.612285	-0.854662	H 5.495708	-4.295676	-1.590301
H -1.349976	-3.221943	2.108563	H 4.798146	-6.640411	-1.040763
H -1.350553	-2.366620	-1.255409	C 0.736126	-6.625240	1.462978
H 0.049716	-4.396380	-2.552461	C 1.340322	-2.264220	2.679369
H 0.018942	-5.232218	1.710949	C -0.518898	-3.291029	1.512594
H 0.738417	-5.851821	-0.616053	C 0.696854	-2.481181	3.909602
O -1.817970	-0.282423	-0.524520	H 2.324648	-1.773333	2.649473
H -0.823829	-0.354579	-0.585264	H -1.164009	-3.510431	2.745291
H -0.800800	-1.031837	-2.772203	H -1.033386	-3.600132	0.590296
C 3.338443	0.144338	-4.204122	C -0.565130	-3.105062	3.946001
H 4.271368	-0.391991	-3.963305	H 1.899770	-2.160002	4.840681
H 2.988262	-0.232999	-5.213058	C -2.156048	-3.968012	2.768720
H 3.574168	1.222534	-4.338307	H -1.092736	-3.272153	4.900655
C -1.359680	2.656066	-2.075991	C -4.927074	-0.982389	-1.578292
C -0.079953	3.232354	-1.982026	C -5.752790	-0.896407	-0.662202
C 0.271536	3.987917	-0.849030	C -6.125425	-2.031374	0.087236
C -0.658240	4.177532	0.088338	C -5.496922	-3.269323	-0.157192
C -1.936351	3.600495	1.093314	C -4.949670	-3.348288	-1.073699
C -2.296995	2.685568	-1.049048	C -4.072888	-2.212588	-1.823151
F 0.813254	3.042311	-1.961957	F -5.850600	-4.360830	0.528646
F -1.686752	1.926318	-3.147345	F -7.117764	-1.945324	0.984224
F -3.524705	2.342135	-1.139694	F -6.359069	-2.744556	-0.455829
F 1.497125	4.521730	-0.754203	F -4.283949	0.110796	-2.241596
F -0.316136	4.876069	1.276531	F -3.788051	-4.501102	-1.252728
F -2.814627	3.750220	1.095082	F -3.042409	-2.279472	-2.690436
			C 4.803752	1.106987	1.175532
			C 4.096315	1.881049	0.239425
			C 4.393583	1.776249	-1.131080
			C 4.590200	0.959831	-1.555250
			C 6.186863	0.204815	-0.614844
			C 5.871743	0.291883	0.754589
			F 3.112864	2.692330	0.651808
			F 4.483519	1.175839	2.474347
			F 6.567309	-0.415908	1.648872
			F 5.760824	0.875816	-2.855978
			F 7.209074	-0.557441	-1.019079